An Accurate Methodology to Identify the Level of Aggregation in Solution by PGSE NMR Measurements: The Case of Half-Sandwich Diamino Ruthenium(II) Salts

Daniele Zuccaccia and Alceo Macchioni*

Dipartimento di Chimica, Università di Perugia, Via Elce di Sotto, 8-06123 Perugia, Italy

Received March 1, 2005

The utility of PGSE NMR measurements in determining hydrodynamic radii (r_H) and volumes (V_H) of small- and medium-size molecules (3 Å < r_H < 6 Å) was evaluated by performing measurements for a variety of pure deuterated solvents and their solutions containing the internal standard TMSS [tetrakis(trimethylsilyl)silane] also in the presence of a variable concentration of **3**BPh_4. It was found that accurate r_H and V_H values can be obtained by introducing in the Stokes−Einstein equation ($D_t = kT/c\pi\eta r_H$) not only the correct values for temperature (T) and viscosity (η) but, particularly, that for the c factor. PGSE NMR measurements were then applied to an investigation of the aggregation tendency of complexes [Ru(η^6-cymene)($R_1R_2NCH_2CH_2NR_1R_2$)Cl]X ($R_1 = R_2 = H$, **1**; $R_1 = H$, $R_2 = H$, **2**; $R_1 = R_2 = Me$, **3**; $X^- = PF_6^-$ or BPh_4^-) in both protic and aprotic solvents with a relative permittivity (ϵ_r) ranging from 4.81 (chloroform-d) to 32.66 (methanol-d_4). Compounds **1** and **2** exhibited a remarkable tendency to aggregate through intercationic N−H···Cl and cation/anion N−H···FPF_5^- hydrogen bonds. In addition to ion pairs, ion triples and ion quadruples were also observed in solution. Compound **3**, having no N-H moiety, showed less tendency to aggregate than **1** and **2**, even though it also afforded ion quadruples in apolar and aprotic solvents. Relative anion−cation orientations and arene conformations were investigated by means of ^{1}H−NOESY and ^{19}F,^{1}H-HOESY NMR spectroscopy. The relative anion−cation position was well-defined, especially for compounds bearing the PF_6^- counterion, and was modulated by the nature of the N,N ligand. A progressive slackening of the contact aggregates was observed in the series **1**−**3** that led to a higher mobility of the anion, as indicated by the observation of less specific interionic NOEs.

Introduction

Diffusion NMR spectroscopy[1] has proven to be a powerful tool for determining molecular size in solution.[2,3] The hydrodynamic radius (r_H) of the diffusing species can be estimated from the experimentally determined self-diffusion translational coefficient (D_t) by taking advantage of the Stokes−Einstein equation:

$$D_t = \frac{kT}{c\pi\eta r_H} \quad (1)$$

where k is the Boltzmann constant, T is the temperature, c is a numerical factor, and η is the solution viscosity. Because the error on D_t is usually lower than 5%, accurate values of r_H can be derived once the three other parameters of eq 1, T, c, and η, are correctly evaluated. While T and η can be measured, the selection of the proper c factor is critical. This is particularly true for medium- and small-size molecules, for which c differs significantly from both 4 (slip boundary conditions) or 6 (stick boundary conditions). To avoid the measurement of T and η and the evaluation of c, an internal standard of known van der Waals radius (r_{VdW}) can be used to determine the proportional constant between D_t and r_H of eq 1.[4,5] Two assumptions are implicit in this procedure: (a) r_{VdW} is a good representation of r_H for the internal standard and (b) the proportional constant for the standard and that for the sample are the same and, since they are in the same solution and experience the same T and η, this means that they have the same c factor. Assumption (a) is usually considered correct.[6,7] Since the c factor substantially depends on the size of the diffusing species, assumption (b) is only respected if the standard and the sample have the same or, at least, comparable dimensions. Otherwise, c has to be evaluated. An acceptable semiempirical estimation

* To whom correspondence should be addressed. E-mail: alceo@unipg.it. Fax: +39 075 5855598. Phone: +39 075 5855579.

(1) Hahn, E. L. *Phys. Rev.* **1950**, *80*, 580−594. Stejskal, E. O.; Tanner, J. E. *J. Chem Phys.* **1965**, *42*, 288. Stilbs, P. *Prog. Nucl. Magn. Reson. Spectrosc.* **1987**, *19*, 1. Price, W. S. *Concepts Magn. Res*. **1997**, *9*, 299. Price, W. S. *Concepts Magn. Res*. **1998**, *10*, 197. Johnson, C. S., Jr. *Prog. Nucl. Magn. Reson. Spectrosc.* **1999**, *34*, 203.

(2) For reviews on applications to organometallic chemistry, see: Valentini, M.; Rüegger, H.; Pregosin, P. S. *Helv. Chim. Acta* **2001**, *84*, 2833. Binotti, B.; Macchioni, A.; Zuccaccia, C.; Zuccaccia, D. *Comments Inorg. Chem.* **2002**, *23*, 417. Pregosin, P. S.; Martinez-Viviente, E.; Kumar, P. G. A. *Dalton Trans.* **2003**, 4007.

(3) For a recent review on the application in supramolecular chemistry, see: Cohen, Y.; Avram, L.; Frish, L. *Angew. Chem., Int. Ed.* **2005**, *44*, 520.

(4) Mo, H.; Pochapsky, T. C. *J. Phys. Chem. B* **1997**, *101*, 4485.

(5) Zuccaccia, C.; Bellachioma, G.; Cardaci, G.; Macchioni, A. *Organometallics* **2000**, *19*, 4663.

(6) (a) Bondi, A. *J. Phys. Chem.* **1964**, *68*, 441. (b) Rowland R. S.; Taylor, R. *J. Phys. Chem.* **1996**, *100*, 7384.

(7) Edward, J. T. *J. Chem. Educ.* **1970**, *47*, 261.

10.1021/om050145k CCC: $30.25
Publication on Web 06/04/2005

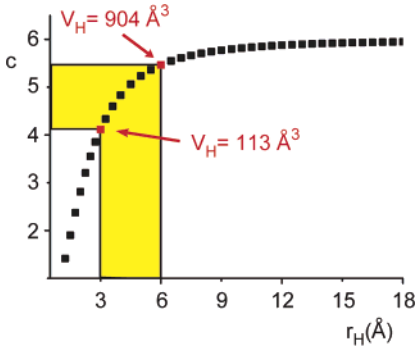

Figure 1. Dependence of the *c* factor of a diffusing particle on the hydrodynamic radius (r_H) in methylene chloride-d_2 according to eq 2.

of *c* can be obtained through eq 2[8] derived from the microfriction theory proposed by Wirtz and co-workers,[9] in which *c* is expressed as a function of the solute-to-solvent ratio of radii.

$$c = \frac{6}{\left[1 + 0.695\left(\frac{r_{solv}}{r_H}\right)^{2.234}\right]} \qquad (2)$$

Combining eqs 1 and 2, the Stokes−Einstein equation, eq 3, is obtained in which D_t depends on both r_H and the hydrodynamic radius of solvent (r_{solv}).

$$D_t = \frac{kT\left[1 + 0.695\left(\frac{r_{solv}}{r_H}\right)^{2.234}\right]}{6\pi\eta r_H} \qquad (3)$$

An example of the dependence of *c* on r_H is reported in Figure 1 for methylene chloride-d_2 (r_{solv} = 2.49 Å). Mononuclear organometallic compounds have a hydrodynamic radius that usually falls in the 3−6 Å range. Therefore, according to Figure 1, *c* varies from 4.1 to 5.5. Consequently, if $c = 6$ is introduced into eq 3, the error on the derived r_H spans from 9% to 32%.

In our laboratory, we have been interested in the aggregation of transition-metal organometallics in solution for several years.[10−13] We are trying to correlate the effect of aggregation on the chemical reactivity[14] with the intermolecular structure. For intermolecular structure, we mean both the relative position of the interacting moieties, determined by NOE (nuclear Overhauser effect) NMR experiments, and the level of aggregation, estimated by PGSE (pulsed field gradient spin−echo) NMR technique. Clearly, when the aggregation level in solution has to be determined through diffusion measurements, the use of an internal standard becomes problematic since the average dimensions of the species present in solution can easily change when solvent or concentration vary and, consequently, the standard cannot be suitable for all circumstances. In such cases eqs 2 and 3 have to be used for evaluating *c* and r_H, respectively.

In this paper, we first show that treating D_t data coming from PGSE NMR measurements with eq 3 leads to a more accurate estimation of r_H with respect to those obtainable using eq 1 with $c = 4$ or 6. Second, we report the PGSE results, treated with the methodology based on eq 3, pertinent to the aggregation of [(arene)Ru(N,N)Cl]X compounds (where N,N = diamine ligands) in various solvents. Finally, for the latter, relative anion−cation orientations and the conformations of cymene, determined by NOE NMR measurements, are also illustrated.

Half-sandwich diamino ruthenium(II) salts were selected in order to contrast their tendency to aggregate with that of analogous diimine complexes, which is remarkable.[12] In addition, even though they have been known for several decades,[15] there has been a renewed interest in them since Sadler and co-workers[16] demonstrated their anticancer activity. This activity seems to be connected to the possibility of such compounds to strongly and selectively bind N7 of guanine and its derivatives, in a physiological environment. In-depth studies[16] have shown that in such binding a crucial role is played by the covalent coordination of N7 on the metal center, π-stacking between the nucleobase and the arene of the complexes, and stereospecific H-bonding between the hydrogen-bond donors (NH functionalities of Ru complexes) and hydrogen-bond acceptors (carbonyl functionalities on nitrogenous base). It appears reasonable that H-bonding and π-stacking, which are responsible for the favorable interaction between DNA and [(arene)Ru(N,N)Cl]X salts, could also lead to self-aggregation of the latter in solution with the possible formation of ion pairs or even higher aggregates.

Results

Synthesis. Complexes [Ru(η^6-cymene)($R_1R_2NCH_2CH_2NR_1R_2$)Cl]X shown in Scheme 1 were synthesized by the reaction of [$Ru_2(\eta^6$-cymene$)_2Cl_2(\mu$-Cl$)_2$] with the appropriate ligand in methanol at room temperature by adding a large excess of $NaBPh_4$ or NH_4PF_6, which caused the precipitation of the desired ruthenium salt.[15] Due to their high solubility in methanol, complexes **2**PF_6 and **3**PF_6 were preferentially synthesized by **2**BPh_4 and **3**BPh_4 through anion metathesis using an equimolar quantity of $TlPF_6$ in methylene chloride.

Of the three possible isomers of complexes **2**X (Scheme 2), differing in the relative orientation of the R substit-

(8) Chen, H.-C.; Chen, S.-H. *J. Phys. Chem.* **1984**, *88*, 5118. Espinosa, P. J.; de la Torre, J. G. *J. Phys. Chem.* **1987**, *91*, 3612.
(9) Gierer, A.; Wirtz, K. *Z. Naturforsch. A* **1953**, *8*, 522. Spernol, A.; Wirtz, K. *Z. Naturforsch. A* **1953**, *8*, 532.
(10) Macchioni, A. *Eur. J. Inorg. Chem.* **2003**, 195. Macchioni, A. In *Perspectives in Organometallic Chemistry*; Screttas, C. G., Steele, B. R., Eds.; The Royal Society of Chemistry: Cambridge, 2003; pp 196−207.
(11) Zuccaccia, C.; Stahl, N. G.; Macchioni, A.; Chen, M.-C.; Roberts, J. A.; Marks, T. J. *J. Am. Chem. Soc.* **2004**, *126*, 1448.
(12) Zuccaccia, D.; Sabatini, S.; Bellachioma, G.; Cardaci, G.; Clot, E.; Macchioni, A.; *Inorg. Chem.* **2003**, *42*, 5465.
(13) Zuccaccia, D.; Clot, E.; Macchioni, A. *New J. Chem.* **2005**, *29*, 430.
(14) For a recent review on ion pairing effect in transition-metal organometallic chemistry, see: Macchioni, A. *Chem. Rev.* **2005**, in press.
(15) Crabtree, R. H.; Pearman, A. J. *J. Organomet. Chem.* **1977**, *141*, 325.
(16) (a) Novakova, O.; Chen, H.; Vrana, O.; Rodger, A.; Sadler, P. J.; Brabek, V. *Biochemistry* **2003**, *42*, 11544. (b) Chen, H.; Morris, R. E.; Sadler, P. J. *J. Am. Chem Soc.* **2003**, *125*, 173. (c) Aird, R. E.; Cumming, J.; Ritchie, A. A.; Muir, M.; Morris, R. E.; Chen, H.; Sadler, P. J.; Jodrell, D. L. *Br. J. Cancer* **2002**, *86*, 1652. (d) Chen, H.; Parkinson, J.; Morris, R. E.; Parson, S.; Coxall, R. A.; Gould, R. O.; Sadler, P. J. *J. Am. Chem Soc.* **2002**, *124*, 3064. (e) Morris, R. E.; Aird, R. E.; Murdoch, Piedad del Socorro; Chen, H.; Cumming, J.; Hughes, N.; Parson, S.; Parkin, A.; Boyd, G.; Jodrell, D. L.; Sadler, P. J. *J. Med. Chem.* **2001**, *44*, 1652.

Scheme 1

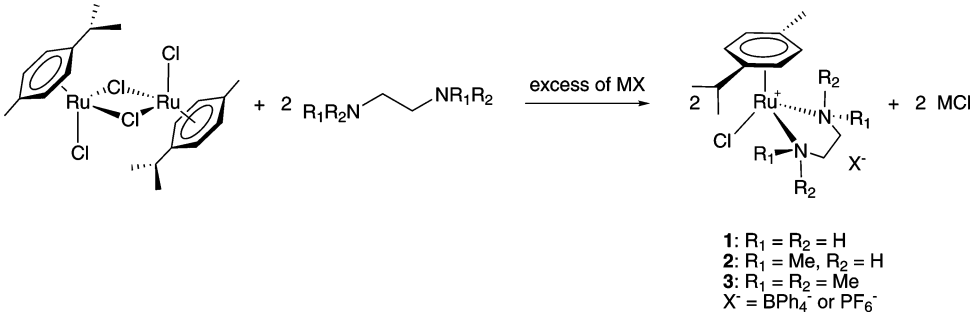

1: $R_1 = R_2 = H$
2: $R_1 = Me$, $R_2 = H$
3: $R_1 = R_2 = Me$
$X^- = BPh_4^-$ or PF_6^-

Scheme 2

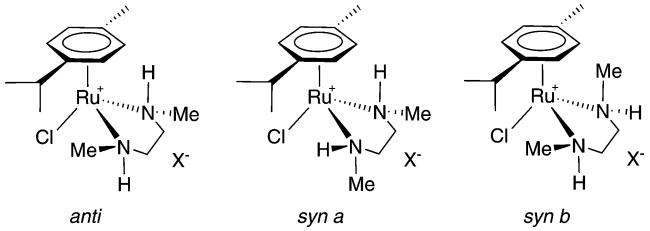

uents, only the *anti* isomer was observed in solution. The metal center in the latter is chiral and, consequently, two enantiomers are present in solution in equal amount.

Evaluation of the Accuracy of PGSE NMR Measurements. (a) Determination of the Hydrodynamic Volumes of Solvents. The goodness of eq 3 was checked by measuring D_t for samples of pure deuterated solvents following the decrease of the signal due to the small percentage of nondeuterated solvent as a function of the gradient strength (G) increases (Experimental Section).

The viscosity values introduced in the modified Stokes−Einstein equation, eq 3, were known from the literature;[17] they were corrected to take into account both the actual temperature[17] and the deuteration of the solvents.[18] The D_t of water, which is necessary to calibrate the gradient intensities, or better, to measure the proportionality constant to obtain D_t (Experimental Section), was also interpolated at the corrected temperature.[19] The D_t values agree with those reported in the literature.[18] Experimental r_H and van der Waals radii (r_{vdW}) of the investigated solvents are reported in Table 1. For aprotic solvents (Table 1, entries 1−3, 5, 8) there is a good agreement between the van der Waals radii, r_{vdW}, and the experimental hydrodynamic radii, r_H. The deviations [$\Delta r/r$ in Table 1, where $\Delta r/r = (r_H - r_{VdW})/r_{VdW}$] are smaller than 4% and comparable to the experimental error of the measurements (Experimental Section). In constrast, the experimental hydrodynamic radii for protic solvents (Table 1, entries 4, 6, 7) are 20−25% larger than the calculated van der Waals radii. This reasonably reflects the self-association of alcoholic solvents. Iterative calculations were carried out using the initially derived hydrodynamic radius r_H value as r_{solv} in the Stokes−Einstein equation, eq 3, and comparing the new r_H value with the old r_H. This process was repeated several times until there was a convergence between the last estimated hydrodynamic radius and the preceding one introduced in eq 3. The resulting hydrodynamic radii (indicated as r_H^{conv} in Table 1) were used to determine the volumes of the diffusing species in protic solvents.

Table 1. Diffusion Coefficients ($10^9 D_t$ m^2 s^{-1}), van der Waals Radii (r_{vdW}), Experimental Hydrodynamic Radii (r_H), and Experimental Hydrodynamic Radii at Convergence (r_H^{conv}) Obtained for Pure Deuterated Solvent (ϵ_r at 25 °C)

		D_t	r_{vdW}	r_H	($\Delta r/r$ %)	r_H^{conv}
1	benzene-d_6 (2.27)	2.02	2.7	2.68	−0.7	
2	chloroform-d (4.81[a])	2.42	2.6	2.65	1.9	
3	CD_2Cl_2 (8.93)	3.37	2.49	2.46	−1.2	
4	2-propanol-d_8 (19.92)	0.47	2.40	2.86	20	3.08
5	acetone-d_6 (20.56)	4.15	2.49	2.54	2.0	
6	ethanol-d_6 (24.55)	0.94	2.25	2.75	22	3.10
7	methanol-d_4 (32.66)	2.12	1.99	2.48	25	2.76
8	DMSO-d_6 (46.45)	0.61	2.63	2.72	3.4	

(b) Determination of the Hydrodynamic Volume of TMSS in Different Solvents. To check the reliability of using r_{vdW} and r_H^{conv} values in eq 3 for aprotic and protic solvents, respectively, PGSE measurements were performed for 0.1 mM solutions of TMSS [tetrakis(trimethylsilyl)silane], whose van der Waals radius is known from the literature (r_{vdW} = 4.28 Å).[20] The experimental r_H and c values are reported in Table 2. Hydrodynamic radii that were derived by setting c equal to 4 or 6 in eq 1 are also reported in Table 2 for comparison. While there is a good agreement between the estimated hydrodynamic radius of TMSS and its van der Waals radius when the proper c factor is used (error < 4%), the use of 6 or 4 in eq 1 leads to errors in the 5−30% range.

The effect of the concentration on viscosity and, consequently, on the derived r_H was checked by performing PGSE NMR measurements for solutions of TMSS (1 mM) in methylene chloride-d_2 containing different amounts of **3**BPh_4. Hydrodynamic radii of TMSS determined by introducing the viscosity of pure solvent in eq 3 or by taking into account the solution viscosity are reported in Table 3. The solution viscosity was calculated by multiplying the viscosity of the pure solvent by a correction factor. The latter was equal to the ratio of the slopes of the straight lines derived by plotting $\log(I/I_0)$ vs G^2 for the resonances relative to nondeuterated solvent residue in pure solvent and in the solution.

(17) *Handbook of Chemistry and Physics*, 67th ed; CRC Press: Boca Raton, FL, 1987.
(18) Holz, M.; Xi-an, Mao; Seiferling, D.; Sacco, A. *J. Chem. Phys.* **1996**, *104*, 669.
(19) Mills, R. *J. Phys. Chem.* **1973**, *77*, 685.
(20) Dinnebier, R. E.; Dollase, W. A.; Helluy, X.; Kümmerlen, J.; Sebald, A.; Schmidt, M. U.; Pagola, S.; Stephens, P. W.; van Smaalen, S. *Acta Crystallogr.* **1999**, *B55*, 1014.

Table 2. Diffusion Coefficients ($10^9 D_t$ m^2 s^{-1}), *c* Factor Values, and Hydrodynamic Radii (r_H) Obtained with Different *c* Factors with Their Respective Percentage Errors, for Solutions of TMSS (0.1 mM) as a Function of Solvent (ϵ_r at 25 °C)

		D_t	*c*	$r_H^{(c)}(\Delta r/r\%)$	$r_H^{(c=4)}(\Delta r/r\%)$	$r_H^{(c=6)}(\Delta r/r\%)$
1	benzene-d_6 (2.27)	0.99	4.7	4.10 (4.2)	4.75 (10)	3.17 (26)
2	chloroform-*d* (4.81[a])	1.07	4.9	4.27 (0.3)	5.21 (21)	3.47 (19)
3	CD_2Cl_2 (8.93)	1.47	5.0	4.22 (1.5)	5.20 (21)	3.47 (19)
4	2-propanol-d_8 (19.92)	0.28	4.4	4.23 (1.2)	4.70 (10)	3.13 (27)
5	acetone-d_6 (20.56)	1.85	4.9	4.21 (1.7)	5.20 (21)	3.46 (19)
6	ethanol-d_6 (24.55)	0.54	4.5	4.25 (0.8)	4.76 (11)	3.17 (26)
7	methanol-d_4 (32.66)	1.04	4.7	4.24 (0.9)	5.00 (16)	3.34 (22)
8	DMSO-d_6 (46.45)	0.29	4.9	4.28 (0.1)	5.21 (21)	3.47 (19)

Table 3. Diffusion Coefficients ($10^9 D_t$ m^2 s^{-1}), *c* Factor Values, and Hydrodynamic Radii (r_H) Obtained with Solvent Viscosity and Solution Viscosity, for Solutions of TMSS (1 mM) in Methylene Chloride-d_2 at Various Concentrations (*C*, mM) of 3BPh$_4$

			solution viscosity		solvent viscosity		
	C	D_t	*c*	$r_H^{(c)}(\Delta r/r\%)$	*c*	$r_H^{(c)}(\Delta r/r\%)$	$r_H^{(c=6)}(\Delta r/r\%)$
1	0.7	1.39	5.0	4.28 (−0.01)	5.1	4.36 (1.8)	3.69 (−14)
3	12	1.34	5.1	4.29 (0.2)	5.1	4.47 (4.4)	3.82 (−10)
4	24	1.35	5.1	4.28 (−0.01)	5.1	4.45 (4.0)	3.80 (−11)
5	56	1.26	5.1	4.29 (0.2)	5.2	4.69 (9.4)	4.06 (5)
6	156	1.05	5.1	4.32 (0.9)	5.4	5.43 (27)	4.96 (15)

From the results reported in Table 3, it can be noted that the hydrodynamic radius of the TMSS is nicely reproduced in all cases if we use the solution viscosity in eq 3. On the contrary, if the increased solution viscosity derived from the addition of the **3**BPh$_4$ salt was not taken into account, r_H would be overestimated and an apparent increased level of aggregation would be deduced. Clearly, the error increases in cases of more concentrated solutions. It is worth noting that if eq 1 with $c = 6$ is used, the two errors derived from considering (a) solvent instead of solution viscosity and (b) 6 instead of the correctly determined *c* factor (which tends to underestimate the hydrodynamic radius) go in opposite directions and can compensate in some cases. For example, for a 56 mM solution of **3**BPh$_4$ in methylene chloride-d_2 (Table 3, entry 5), r_H of TMSS is nicely reproduced (error of 0.2%) if the solution viscosity and the correct *c* factor are introduced in eq 3. The utilization of the solvent viscosity and the correct *c* factor affords a much higher error (9.4%), but if the solvent viscosity and the *c* factor corresponding to the stick boundary condition ($c = 6$) are introduced in eq 3, the two errors partially compensate (5%).

PGSE Measurements for Arene Ruthenium Complexes Bearing Diamine Complexes. ^{1}H and ^{19}F-PGSE NMR experiments were carried out for complexes **1**, **2**, and **3** in different solvents, with a relative permittivity (ϵ_r) ranging from 4.81 (chloroform-*d*) to 32.66 (methanol-d_4), using TMSS as internal standard. PGSE measurements allowed the translational self-diffusion coefficients (D_t) for both cationic (D_t^+) and anionic (D_t^-) moieties (Table 4) to be determined. By applying eq 3, the average hydrodynamic radii and *c* factors for the anionic and cationic moieties were measured (Table 4). Their volumes were obtained from the average hydrodynamic radii of the aggregates, which were assumed to be spherical. The volumes of the diffusing particles were then compared with the van der Waals volumes of ion pairs known from the solid state (Experimental Section). The ratios between the apparent volume of the cationic or anionic moieties and that of the ion pairs, N^+ and N^-, respectively, are reported in Table 4. They represent a sort of aggregation number. Of course, a distribution of ionic species is present in solution; consequently N^+ and N^- indicate which is the apparent average aggregation number of the ionic moieties. For example, if they are both equal to 1 or 2, this means that either ion pairs or ion quadruples, i.e., "$(Ru^+X^-)_2$", are the predominant species in solution, respectively. Less intuitive is the interpretation of *N* values when odd aggregates are significantly present in solution, i.e., when $N < 1$ or $N^+ \neq N^-$, because of the different volumes of the single ionic fragments. In our cases, they are[6,16e] $N^+ = 0.44$ and $N^- = 0.56$ for **1**BPh$_4$, $N^+ = 0.78$ and $N^- = 0.22$ for **1**PF$_6$, $N^+ = 0.47$ and $N^- = 0.53$ for **2**BPh$_4$, $N^+ = 0.81$ and $N^- = 0.19$ for **2**PF$_6$, $N^+ = 0.50$ and $N^- = 0.50$ for **3**BPh$_4$, and $N^+ = 0.83$ and $N^- = 0.17$ for **3**PF$_6$. If N^+ and/or N^- are larger than the previously indicated aggregation number of free ions, then ion pairing and/or higher aggregation occurs.

All measurements indicated that a certain level of aggregation was always present and that it was strongly affected by the choice of ligand, solvent, and concentration. In constrast, the level of aggregation was not very sensitive to the nature of the counterion.

(a) Ligand Effect on Aggregation: The Role of the NH Group. The aggregation tendency of **1**PF$_6$, **2**PF$_6$, and **3**PF$_6$ was studied in methylene chloride-d_2 at the same concentration (4 mM, entries 1, 4, 12 of Table 4). The aggregation tendency follows in the order **1** > **2** ≈ **3**. Compound **1**PF$_6$, which contains two NH$_2$ functionalities, prevalently forms ion quadruples in solution, while the introduction of two methyl groups (**2**PF$_6$) lowers the aggregation number, from 1.9 to 1.5 for N^+ and from 1.9 to 1.4 for N^-. Compound **3**PF$_6$, which contains two NMe$_2$ functionalities, shows less aggregation tendency than **1**PF$_6$, but, interestingly enough, it has the same N^+ and similar N^- as compound **2**PF$_6$. The difference between N^+ and N^- increases on passing from NH$_2$ functionalities to NMe$_2$, indicating that the presence of methyl tends to slacken the anion−cation adducts. Another important comparison is the trend of the aggregation number in methylene chloride-d_2 in the saturated solutions (entries 1, 5, 25). N^+ and N^- are both equal to 1.9 and 1.5 for **1**PF$_6$ and **2**PF$_6$, respectively, while they are equal to 2.0 and 1.9 for **3**PF$_6$. Probably the presence of methyl groups not only induces a broadening of anion−cation adducts that disfavors the formation of aggregates (**1**PF$_6$ vs **2**PF$_6$) but tends to increase the solubility of the adducts. The increased solubility for **3**PF$_6$ permits increasing the concentration by about 30 times; this could force the ion-pairs/ion-quadruples equilibrium to shift to the right

Table 4. Diffusion Coefficients ($10^{10}D_t$ m^2 s^{-1}), Hydrodynamic Radii (r_H, Å), *c* Factors, and Aggregation Numbers (*N*) for Compounds 1, 2, and 3 as a Function of Solvent (ϵ_r at 25 °C) and Concentration (*C*, mM)

		D_t^+	D_t^-	r_H^+	c_H^+	r_H^-	c_H^-	N^+	N^-	*C*
	1PF_6 (V_{ip} = 283)									
1	CD_2Cl_2 (8.93)	11.0	10.9	5.1	5.3	5.0	5.3	1.9	1.9	4
2	2-propanol-d_8 (19.92)	2.0	2.6	5.0	4.9	4.3	4.5	1.9	1.1	4
	1BPh_4 (V_{ip} = 507)									
3	CD_2Cl_2 (8.93)	8.5	8.8	6.2	5.6	6.1	5.5	2.0	1.9	4
	2PF_6 (V_{ip} = 315)									
4	CD_2Cl_2 (8.93)	10.9	11.4	4.8	5.3	4.7	5.2	1.5	1.4	4
5	CD_2Cl_2 (8.93)	11.6	11.4	4.8	5.3	4.8	5.3	1.5	1.5	6[b]
	2BPh_4 (V_{ip} = 540)									
6	CD_2Cl_2 (8.93)	9.1	8.9	5.7	5.5	5.8	5.5	1.4	1.5	4
7	CD_2Cl_2 (8.93)	8.6	8.6	5.8	5.5	5.8	5.5	1.5	1.5	12
8	CD_2Cl_2 (8.93)	8.3	8.3	5.9	5.5	5.9	5.5	1.6	1.6	15[b]
	3PF_6 (V_{ip} = 347)									
9	chloroform-*d* (4.81[a])	7.5	7.6	5.5	5.3	5.4	5.3	2.0	1.9	1.15[b]
10	CD_2Cl_2 (8.93)	11.3	11.9	4.8	5.2	4.7	5.2	1.3	1.1	0.7
11	CD_2Cl_2 (8.93)	10.9	11.7	4.9	5.2	4.7	5.2	1.4	1.2	2.7
12	CD_2Cl_2 (8.93)	11.2	11.6	4.9	5.3	4.8	5.3	1.5	1.3	4
13	CD_2Cl_2 (8.93)	9.8	10.7	5.1	5.4	4.8	5.2	1.7	1.4	18
14	CD_2Cl_2 (8.93)	9.4	9.9	5.2	5.4	5.1	5.3	1.8	1.6	34
15	CD_2Cl_2 (8.93)	8.6	9.2	5.4	5.4	5.1	5.3	1.9	1.7	80
16	CD_2Cl_2 (8.93)	8.4	8.7	5.6	5.4	5.4	5.4	2.1	2.0	115[b]
17	acetone-d_6 (20.56)	16.2	25.3	4.8	5.2	3.6	3.7	1.3	0.5	4
18	methanol-d_4 (32.66)	8.8	12.9	5.0	5.1	3.9	4.5	1.5	0.7	6[b]
	3BPh_4 (V_{ip} = 571)									
19	chloroform-*d* (4.81[a])	6.3	6.3	6.4	5.5	6.4	5.5	1.9	1.9	0.5[b]
20	CD_2Cl_2 (8.93)	10.7	9.8	5.1	5.4	5.3	5.3	1.0	1.1	0.7
21	CD_2Cl_2 (8.93)	9.9	9.2	5.4	5.4	5.7	5.5	1.2	1.4	2.7
22	CD_2Cl_2 (8.93)	9.1	8.6	5.6	5.4	5.9	5.5	1.3	1.5	12
23	CD_2Cl_2 (8.93)	8.6	8.3	5.8	5.5	6.0	5.5	1.4	1.6	24
24	CD_2Cl_2 (8.93)	7.8	7.6	6.0	5.5	6.1	5.5	1.6	1.7	56
25	CD_2Cl_2 (8.93)	6.1	6.0	6.3	5.6	6.4	5.6	1.9	2.0	156
26	acetone-d_6 (20.56)	14.7	14.8	5.0	5.2	5.0	5.2	0.9	0.9	4

[a] 20 °C. [b] Saturated solution.

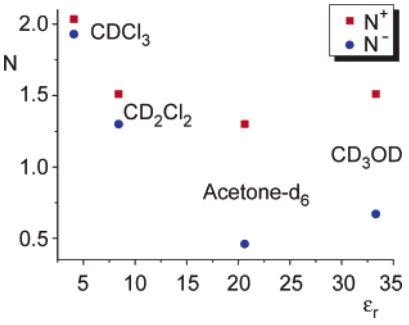

Figure 2. Trends of the aggregation numbers (N^+ and N^-) of compound **3**PF_6 as a function of the relative permittivity of the solvent.

even if ion quadruples are energetically less favored than in **1**,**2**PF_6.

(b) Solvent Effect on Aggregation. The aggregation tendency of **3**PF_6 was studied in several solvents. The dependence of N^+ and N^- on ϵ_r is reported in Figure 2. It clearly shows that N^+ and N^- increase as ϵ_r decreases, reaching the maximum value of 2 for chloroform-*d* where quadrupoles are mainly present. The minimum level of aggregation is observed in acetone-d_6, where still a significant amount of ion pairs is present. Another clear trend shown in Figure 2 is that the N^+ value is higher than that of N^- with a difference that increases with ϵ_r up to acetone-d_6. Surprisingly, a comparison between acetone-d_6 (ϵ_r = 20.56) and methanol-d_4 (ϵ_r = 32.66) indicates that the aggregation tendency is higher in the latter.

(c) Concentration Effect on Aggregation. The effect of concentration was investigated for complex **3**X (X = BPh_4 and PF_6) in methylene chloride-d_2. Data are reported in Table 4, entries 10−16 for **3**BPh_4 and entries 20−25 for **3**PF_6. As expected, the aggregation increased with the concentration, but it is significant even at the lowest concentration considered (0.7 mM), for which the aggregation numbers were higher than 1 for both complexes.

Scheme 3

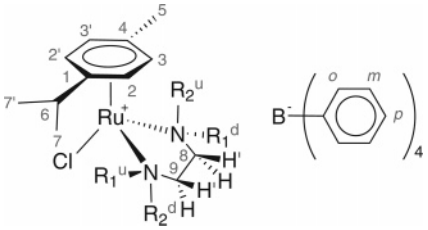

Intramolecular Characterization in Solution: Conformational Analysis of Cymene Rotation through Intramolecular NOE NMR Experiments. All complexes **1**−**3** were characterized in solution by ^{1}H, ^{13}C, and ^{19}F NMR spectroscopies. Data are reported in the Experimental Section. Numbering of carbon and proton resonances is illustrated in Scheme 3.

The higher symmetry of **1** and **3** complexes makes the normal and prime of cymene protons and the two 8H′/9H′ and 8H/9H couples magnetically equivalent. This reduces the number of observed NMR signals and also the availability of spatial "reporters" in the cationic moiety. As a consequence, the results related to complexes **2** will have a dominant position in the following considerations on arene orientations and relative anion−cation positions.

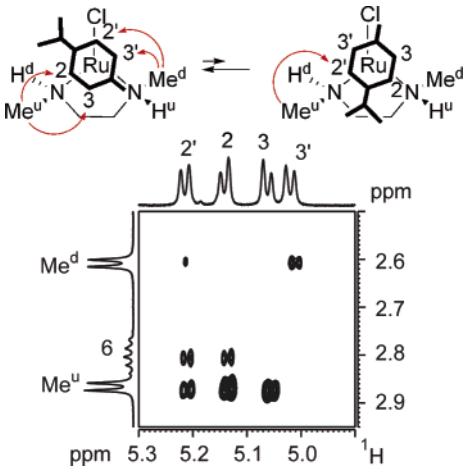

Figure 3. Section of ^{1}H-NOESY NMR spectrum (400.13 MHz, 296 K, methylene chloride-d_2) of complex **2**BPh_4 showing the different interactions of Me^u and Me^d with cymene protons.

From the ^{1}H, ^{13}C, ^{1}H-COSY, ^{1}H-NOESY, ^{1}H,^{13}C-HMQC NMR, and ^{1}H,^{13}C-HMBC NMR spectroscopies it is rather easy to group the proton and carbon resonances belonging to the different fragments. On the contrary, the distinction between the resonances of (1) the methylene protons, (2) the R groups bonded to the nitrogen, and (3) the cymene ligands and the determination of the preferred conformers of cymene are two strictly interlocked and difficult issues that, nevertheless, can be settled by means of ^{1}H-NOESY experiments, as detailed in the following sections.

(a) Complex 2BPh$_4$. As reported in Figure 3, the ^{1}H-NOESY spectrum shows that the dipolar interactions between the cymene protons and one N-Me^u group (labeled u just because it points up toward the cymene) have higher intensities than the analogous one of the other methyl Me^d protons (d stands for down). The two H^d and H^u broad resonances, which are scalar coupled with the methyl Me^u and Me^d, respectively, also show different dipolar interactions with cymene protons. Only the NOEs between the H^u and cymene resonances are visible. An in-depth analysis of the section of ^{1}H-NOESY spectrum reported in Figure 3 shows that the intensity of the NOEs between Me^u and cymene protons follows the order $2 \approx 3 > 2' \gg 3'$. In addition, Me^d gives a medium-size NOE with 3′ and a weak NOE with 2′.

These observations are consistent with the main presence of a preferential orientation of the cymene in which 5-Me is directed toward the nitrogen atom bearing proton H^u with the 7-*i*Pr group located in the nonhindered region between the other nitrogen atom and chlorine (Figure 3). On the other hand, this cymene orientation does not explain the NOE between Me^u and 2′, which has a higher intensity than those of 6 with 2 and 2′. The other orientation with the 5-Me directed toward the chlorine (Figure 3) must be present in solution, even in a limited percentage, to maintain the observed specificity. In Figure 3 the two cymene orientations are reported as eclipsed because such a situation has been observed for compound **1**PF_6 in the solid state.[16e] However, our NOE analysis does not indicate for certain if the preferred orientations are eclipsed or staggered.

The latter criterion for determining the preferential orientation of the cymene (based on the differential Me^u and Me^d/2, 2′, 3, 3′ NOE intensities) is strengthened by the observations that the H^u proton affords a strong NOE with 5-Me cymene protons, while no interaction is present with 6 and 7 (Supporting Information).

Once the R resonances bonded to N have been assigned, it is then possible to assign the four methylene protons due to their selective dipolar interactions; the proton labeled 8′ interacts only with H^u proton and proton 9 interacts only with H^d (Supporting Information). Finally, the ^{1}H,^{13}C-HMQC NMR spectrum shows the scalar coupling of pair 8 and 8′ (and also 9 and 9′) with the same carbon, and so the four methylene protons are assigned (Supporting Information).

(b) Complex 2PF$_6$. The selective dipolar interactions of R groups with cymene protons for this complex also indicate that the conformation with the methyl group oriented toward the H^u proton is more populated than the others, analogous to **2**BPh_4.

(c) Complexes 1X and 3X. In complexes **1** and **3**, 2 and 3 cymene protons are magnetically equivalent (Scheme 3). Consequently, information about the conformation of the cymene is difficult to obtain from ^{1}H-NOESY NMR spectra. Selective dipolar interactions are observed between the protons of R^u and the protons of cymene, while very weak (R = Me) or no (R = H) NOEs are present between the latter and the R^d protons. For compound **1**, the presence of stronger interaction between H^u and 5 with respect to H^u and 2 or 3 suggests that in the preferential orientation of the cymene 5-Me is directed toward the nitrogen atom bearing proton H^u. For compound **3**, the NOE between Me^u and 3 is twice as intense as that between Me^u and 2. This suggests that 5-Me is directed toward the nitrogen atom (as we have seen for complexes **2** and **3**) but is in a more central position with respect to the two N arms, probably due to the steric hindrance of the methyl groups. Once the two different resonances of the R groups are assigned, the two methylene protons (normal from prime) can be distinguished through considerations similar to those made for complex **2**.

Interionic NOE NMR Measurements. The relative anion−cation orientations in solution for complexes **1**−**3**X were studied by detecting dipolar interionic interactions in the ^{19}F,^{1}H-HOESY ($X^- = PF_6^-$) and ^{1}H-NOESY ($X^- = BPh_4^-$) NMR spectra at room temperature (296 K). The following solvents, differing in both relative permittivity and nature, were taken into account: methylene chloride-d_2 ($\epsilon_r^{25°C} = 8.93$), 2-propanol-d_8 ($\epsilon_r^{25°C} = 19.92$), and methanol-$d_4$ ($\epsilon_r^{25°C} = 32.66$). In some cases, after having evaluated the longitudinal relaxation times (Experimental Section), quantitative NOE experiments (mixing time = 150 ms, recycle time = 10 s) were carried out and the derived data were treated taking into account that the volumes of the NOE cross-peaks are proportional to $(n_I n_S/n_I + n_S)$ where n_I and n_S are the number of equivalent I and S nuclei, respectively (Table 5).[21] The preferred relative anion−cation orientations that were deduced from the observed interionic NOEs depended very little on solvent, while

(21) Macura, S.; Ernst, R. R. *Mol. Phys.* **1980**, *41*, 95.

Table 5. Relative NOE Intensities Determined by Arbitrarily Fixing at 1 the Intensity of the NOE(s) between the Anion Resonances (*o*-H in the Case of BPh_4^-) and the Methyl (5) of Cymene

		2BPh_4[a]			**3**PF_6	
	1PF_6[a]	*o*	*m*	**2**PF_6[a]	*a*	*b*
2′	2.7	1.7	0.2	0	1	0.9
2		0.4	0.2	1.1		
3	3.0	0.8	0.2		1.7	1.4
3′		1.4	0.3	*c*		
5	1	1	0.4	1	1	1
7	0.4	0.1	0.1	0.5	0.4	0.6
7′				0		
8′	1.2	0.4	0.3	2.2	1.1	1.4
8		0.3	0.1	0	0.7	1
9′				1.3		
9		0.4	0.2	0		
H^u	3.2	0.3	0.5	2.5[d]		
Me^u		0.2	0.2	0.3	1.6	1.5
H^d	0	0	0	0		
Me^d		0.4	0.2	1.2	0.5	0.9

[a] In methylene chloride-d_2 at 296 K. [b] In methanol-d_4 at 296 K. [e] Difficult to quantitatively evaluate due to overlap with H^u. [d] Probably overestimated due to the superimposition of 3′.

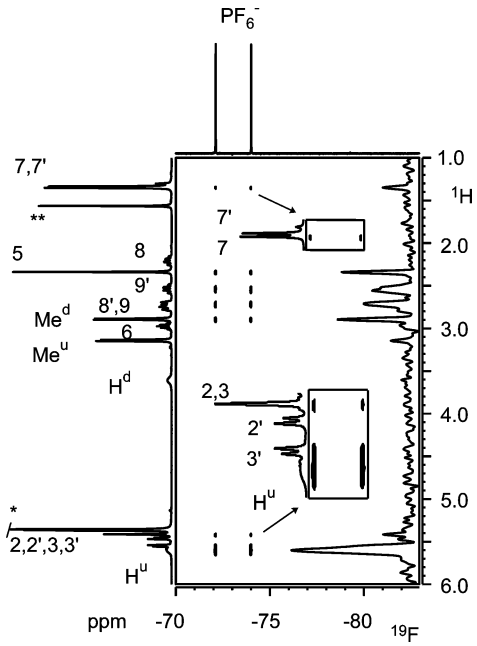

Figure 4. Sections of $^{19}F-^1H$-HOESY NMR spectrum (376.65 MHz, 296 K, methylene chloride-d_2) of complex **2**PF_6. * denotes the resonance due to a residue of non-deuterated solvent. ** denotes the resonance of H_2O.

they were remarkably affected by the nature of the counterion and the R groups bonded to the nitrogen atoms.

(a) $X^- = PF_6^-$. For complex **2**, strong NOE contacts were observed between F atoms of the counterion and 8′, 9′, H^u, and Me^d resonance (Table 5 and Figure 4). Medium-size NOEs were also detected with 2−3, 3′, 5 cymene resonances, while weak NOEs were observed with 7 of the isopropyl group of cymene and with Me^d. The anion did not show any interaction with 2′, 7′, 8, and 9 protons. It is interesting to notice that the anion "sees" all the cymene protons with the exception of 7′ and 2′ (see the expansions in Figure 4). As for the anion interactions with diamine protons, the protons labeled as up or prime "see" the anion, while among the others only Me^d interacts with it. All these observations indicate that PF_6^- is located above the two methylene carbons and the two amine nitrogen moieties and it is shifted toward the less hindered N-arm having the R-group pointing toward the chlorine atom. From this position, the anion can interact with the "prime" cymene protons oriented far away from the chlorine. The detected dipolar interaction with 3′ can be explained by the presence of the other cymene orientation described in the previous section.

In the cases of complexes **1** and **3**, the location of the counterion was necessarily less defined because of the magnetic equivalence of the two sides of both cymene and the N,N ligand. Despite this, for compound **1**, selective dipolar interactions were observed as far as the diamine resonances are concerned; that is, only the prime or up protons showed NOEs with the counterion. The 2 and 3 aromatic cymene resonances interacted dipolarly with the counterion with the same strength as PF_6^-/H^u in **1**PF_6 (3.0 vs 2.7 and 3.2 in Table 5), while in compound **2**, the former interactions were less intense (1.1 vs 2.5 in Table 5). On the contrary, for complex **3** nonnegligible interionic contacts were observed between the counterion and the methylene protons that point far away from the cymene (H8) and Me^d (Table 5). As a consequence, it can be concluded that in complex **1** the anion is located in a more central position with respect to the N,N ligand than in **2** because **1** has equally hindered N-arms; nevertheless, the anion is still located above the two methylene carbons and the two amine nitrogen moieties (CCNN) that are closer to the aromatic cymene resonance. In complex **3**, the anion is also located in a central position, but the presence of methyl groups on both nitrogen atoms probably moves the anion away from the cymene and also makes the position below the CCNN moiety accessible.

(b) $X^- = BPh_4^-$. For this anion, much stronger NOEs were observed between the anion and all cymene and methylene protons. As can be seen from Table 5, the NOE intensities of 8 and 9 with *o*-H were comparable to or even higher than those of 8′ and 9′. The same situation was found for cymene resonances (compare 2′ and 3′ with respect to the 2 and 3). It is possible that the voluminous BPh_4^- anion cannot approach the small cavity formed by the cymene and N,N ligand. As a consequence, the anion can locate on the side of the N,N ligand or above cymene. The energies of the two relative anion−cation orientations may differ very little. Another possibility is that the counterion may assume an intermediate position with one phenyl above the cymene and another directed toward the ligand. Finally, the interionic contacts of *o*-H and *m*-H resonances and cationic protons have completely different intensity trends. NOEs between *m*-H and cationic protons are less intense that those of *o*-H, but the intensity depends very little on the type of cationic protons (Table 5), while *o*-H shows NOE intensities that are strongly affected by the type of cationic protons.

Discussion

Methodology for Obtaining Accurate r_H and V_H Values by PGSE NMR Measurements. The results of PGSE NMR measurements carried out on pure solvents (Table 1), TMSS solutions in various solvents (Table 2), and TMSS in methylene chloride-d_2 at vari-

able concentrations of **3**BPh_4 (Table 3) indicate that accurate r_H and V_H values can be obtained for medium-size molecules by treating the D_t data with eq 3. Our findings show that the utilization of the van der Waals radius instead of the hydrodynamic radius of solvent (r_{solv}) in eq 3 is a good approximation only for aprotic solvents. For protic ones, the r_{solv} to be introduced in eq 3 can be derived through an iterative process starting from $r_{solv} = r_{VdW}$ and then using the derived hydrodynamic radius, r_H, value as r_{solv} until there is a convergence between the last two derived r_H values. By using the latter hydrodynamic radius (r_H^{conv}) as r_{solv} in eq 3 for protic solvents, there is good agreement between the found r_H and the van der Waals radius of TMSS (entries 4, 6, and 7 in Table 2). The viscosity value to be introduced in eq 3 has to be corrected by multiplying the viscosity value of pure deuterated solvents, at the proper temperature, by a factor that is the ratio of the diffusion coefficients of an internal standard (TMSS or the solvent itself) in the solution and in the pure solvent.

Since the reliability of eq 3 has been checked, we here propose a simplified methodology for obtaining accurate r_H values by performing PGSE measurements of the sample of interest containing an internal standard (that can also be the solvent itself). From eq 1, the ratio of the D_t coefficients for the two species is equal to

$$\frac{D_t^{sa}}{D_t^{st}} = \frac{c^{st} r_H^{st}}{c^{sa} r_H^{sa}} \qquad (4)$$

where sa and st stand for sample and standard, respectively. According to eq 2, $c = f(r_{solv}, r_H)$. Since the D_t ratio is measured and r_{solv} and r_H^{st} are known, or can be measured as illustrated above, the only unknown parameter in eq 4 is r_H^{sa}, which can be derived without having to take into account the solution viscosity or temperature. In addition, if the absolute D_t value of the sample is not needed, it is not even necessary to calibrate the gradient strength.

Interionic Structure of Diamino Ru(II) Salts. PGSE NMR investigations reveal that complexes **1**−**3** have a marked tendency to form not only ion pairs but also higher aggregates (up to ion quadruples). The main factor that determines aggregation is the possibility of N-H groups of the diamine ligand to form hydrogen bonds (HBs) with the PF_6^- anion and with the Ru-Cl moiety of another cationic unity. Clearly, this is not the only cause of aggregation since even when N-H groups are not present (as in compound **3**) and the anion is BPh_4^-, ion pairs and ion quadruples may still form (entries 19−25 in Table 4).

Compounds **1** and **2** can form ion quadruples through a [1 × 1] network of intercationic HBs between Ru-Cl and the N-H groups that point down as observed in the solid state for **1**PF_6 (Figure 5).[16e] N-H moieties that point up toward the cymene are committed in HBs with the anion as observed in the solid state for **1**PF_6 (Figure 5) and in solution for **1**PF_6 and **2**PF_6 by means of our interionic NOEs measurements. Interestingly, while ion quadruples are the predominant species in saturated solutions of compound **1** in apolar and aprotic solvents (entries 1 and 3 of Table 4), in the same conditions, compound **2** leads to equimolar solutions of ion pairs and ion quadruples ($N^+ \approx N^- \approx 1.5$, entries 4−8 of Table 4). Since the tendency to afford intercationic HBs of **1** and **2** should be similar, this different behavior could be due to the nucleation process that, in the case of **1**, could go through the association of ion quadruples, while in the case of **2**, could involve an ion quadruple and an ion pair. Even though this issue is highly speculative, simple modeling processes indicate that two ion quadruples can favorably interact in **1** using the N-H moieties not involved in the formation of ion quadruples, while in **2**, this is not possible because of the presence of the N-Me groups. To obtain information about the relative force of the HB networks that hold the two cations and the cation and the anion together, PGSE measurements in 2-propanol-d_8 were performed for **1**PF_6 (entry 2 in Table 4). The results clearly indicate that ion triples **1**$_2PF_6^+$ and PF_6^- are the predominant species in solution. The theoretical N^+ and N^- values for a solution containing only **1**$_2PF_6^+$ and PF_6^- are 1.8 and 1.0, respectively; these values are very similar the observed ones ($N^+ = 1.9$ and $N^- = 1.1$, entry 2 in Table 4). Since the pattern of interionic NOEs is not different from that in other aprotic solvents, it is reasonable to assume that the observed ion triples have the "PF_6-$RuRu^+$" structure; that is, they derive from the dissociation of an anion from the ion quadruples without destroying their structures. This means that for an ion quadruple in a solvent such as 2-propanol-d_8, that is suitable to solvate anions,[22] it is preferable to dissociate an anion rather than form two ion pairs. In agreement with these results, neutral catalysts for transfer hydrogenation in 2-propanol-d_8 exist mainly as dimers and the tendency to form dimers is higher than that of compounds **1** and **2**.[13]

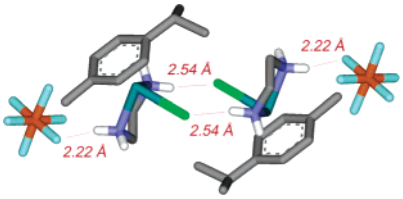

Figure 5. [1 × 1] network of hydrogen bonds between Cl and NH in **1**PF_6 that connects two cationic Ru(II) moieties in the solid state (from ref 16e). Interionic NH···FPF_5^- HBs are also shown.

The lower tendency of compound **3**, which has no N-H group, to afford ion pairs and ion quadruples is intriguing and in agreement with previous results.[12] NOE investigations show that anion−cation interactions are weaker than in **1** and **2** and the anion now also interacts with protons 8 and 9 and with Me[d]. This indicates that less intimate ion pairs are present in solution with a consequent increased dipole moment. In apolar solvents at high concentrations, these ion pairs with elevated dipole moment may persist in solution by reducing their dipole moment through the formation of ion quadruples (entries 16 and 25 in Table 4). Finally, when the ϵ_r of aprotic solvents increases, the aggregation level of **3**PF_6 decreases, while the difference between N^+ and N^- increases (Figure 2) in agreement with previous studies.[12] Interestingly, in methanol-d_4 the aggregation level is higher than in the less polar acetone-d_6 (entries 17, 18 in Table 4). In the former solvent the N^+ and N^-

(22) Reichardt, C. *Solvents and Solvent Effect in Organic Chemistry*; Wiley-VCH: Weinheim, 2003.

values are 1.5 and 0.7, respectively, which suggests that ion triples, analogous to those observed in 2-propanol-d_8, are significantly present. Ion triples in methanol-d_4 have the anion PF_6^- in the usual position as deduced by the observation of heteronuclear NOEs in the $^{19}F,^1H$-HOESY experiments. In this respect, it must be said that anion−cation interionic NOEs were observed in all solvents. The same NOEs were detected also with similar relative intensities (see for example columns a and b in Table 5 pertinent to compound **3**PF_6). For any particular compound, the absolute intensity of NOEs was higher in solvents where a higher percentage of intimate aggregates was present.

Conformational Analysis of Cymene Rotation through NOE NMR Experiments. The arene orientation in half-sandwich arene complexes has been investigated extensively in the solid state.[23] The staggered conformations are usually favored[24−27] but the eclipsed ones have been observed in some cases.[28,29]

In solution, restricted rotation about the arene metal bond has rarely been observed.[30] Theoretical investigations indicate that the rotational energetic barrier of the arene ligand is usually low (10.6 kJ mol^{-1} in [(η^6-C_6H_6)-RuB(pz)$_3$]PF_6[23] and 15.5−19.7 KJ mol^{-1} for [η^6-(C_6H_6)-Cr(CO)$_3$][31]). This means that eclipsed, staggered, or intermediate conformations are all accessible. NOE experiments have been used to determine the arene orientation in solution.[16d,32−34] Sadler and co-workers have described the behavior of the arene in the complex [(η^6-arene)RuY(en)]X where en = ethylendiamine, arene = biphenyl, tetrahydroanthracene, dihydroanthracene, and Y = 9EtG- N7 (guanine base coordinate with N7) or their parent Cl.[16d] In all cases, except for the compound with biphenyl and Cl, in the solid state the arene orients the substituent toward the region between the chlorine or guanine base and one nitrogen of the ligand. A similar situation was found in solution by means of NOESY experiments.

Our NOE experiments for complexes **1**, **2** and **3** show that the conformation of the arene depends on the R substituent of the nitrogen ligand.

In the solid state,[16e] complex **1**PF_6 shows an eclipsed conformation with the cymene methyl close to the nitrogen (1 in Figure 6); in this configuration, the bulky isopropyl group occupies the free region of space between Cl and NR_1R_2. In solution, the cation structure appears to be similar due to the NOE contacts between H^u and 5-Me and the absence of the contact between H^u and 7-*i*Pr. However, this analysis does not allow the orientations ranging from eclipsed to staggered in the δ interval (1 in Figure 6) to be distinguished. A small percentage of the eclipsed or staggered conformation with methyl above the Cl (3 in Figure 6), in which the isopropyl group is between the NH functionalities, must be present. The other 2 and 4 conformations were not observed, probably because they are less stable than the 1 and 3 due to the steric repulsion between bulky isopropyl group and the ligand.

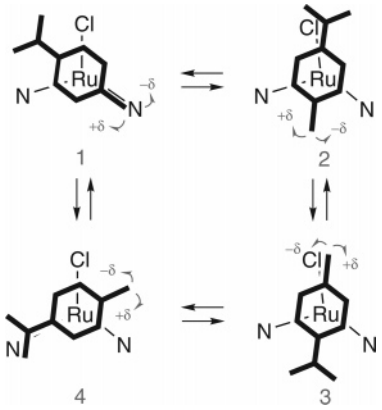

Figure 6. Four possible eclipsed (n) conformers of cymene and their relative staggered conformations ($\pm\delta$).

The two additional "*anti*" methyl groups in complex **2**PF_6 increase the number of observed NMR signals, making more spatial reporters in the cationic moiety available for investigating the arene conformation. Even in this case, the preferential orientation of the cymene is with the 5-Me directed toward the nitrogen atom bearing proton (H^u) and, consequently, the 7-*i*Pr group is located in the nonhindered region between the other nitrogen atom and chlorine (1 in Figure 6). The other orientation with the 5-Me directed toward the chlorine (3 in Figure 6) must still be present in solution even if at a lower percentage in order to maintain the observed specificity of NOE contacts. The conformation in which the 5-Me is directed toward the nitrogen bearing Me^{up} is probably not present due to the steric hindrance of the methyl.

The complex **3**PF_6, where every N atom has two methyl groups, the conformers 1 and 4 of Figure 6 are not stable, probably due to the steric hindrance between NMe_2 and 5-Me or 7-*i*Pr. Of the remaining conformers 2 and 3, the former is the preferred one, as indicated by the NOE between Me^u and protons 3 that is twice as intense as that of the Me^u-2 NOE.

In summary, NMR data indicate that arene orientation in complexes **1**−**3** is mainly dictated by steric effects and, in particular, by the minimization of the steric repulsion between 5-Me and 7-*i*Pr groups and the ligands. As a consequence, when protons are present in the N-arms, as in complex **1**, conformer 1 is the most abundant, but a small percentage of 3 is present. For complex **3**, when the steric hindrance of N-arms is considerable, 5-Me and 7-*i*Pr are directed toward Cl and conformer 2, having 7-*i*Pr close to Cl, is favored.

These results are in perfect agreement with the results reported by Sadler and co-workers;[16d] in fact,

(23) (a) Bhambri, S.; Bishop, A.; Kaltsoyannis, N.; Tocher, D. A. *J. Chem. Soc., Dalton Trans*. **1998**, 3379. (b) Albrigth, T. A. *Acc. Chem. Res.* **1982**, *15*, 149.
(24) Bailey, M. F.; Dahl, L. F. *Inorg. Chem*. **1965**, *4*, 1298.
(25) Koshland, D. E.; Myers, S. E.; Chesick, J. P. *Acta Crystallogr., Sect. B* **1977**, *B33*, 2013.
(26) Bennet, M. A.; Robertson, G. B.; Smith, A. K. *J. Organomet. Chem*. **1972**, *43*, C41.
(27) Restivo, R. J.; Ferguson, G.; O'Sullivan, D. J.; Lalor, F. J. *Inorg. Chem*. **1975**, *12*, 3046.
(28) (a) Iverson, D. J.; Hunter, G.; Blount, J. F.; Damewood, J. R., Jr.; Mislow, K. *J. Am. Chem. Soc.* **1981**, *103*, 6073. (b) Hunter, G.; Blount, J. F.; Damewood, J. R.; Iverson, D. J.; Mislow, K. *Organometallics* **1982**, *1*, 448.
(29) Sledle, A. R.; Newmark, R. A.; Pignolet, L. H.; Wang, D. X.; Albright, T. A. *Organometallics* **1986**, *5*, 38.
(30) Albrigth, T. A.; Hoffmann R.; Tse J. C.; D'Ottavio T. *J. Am. Chem. Soc.* **1979**, *101*, 3812.
(31) Braga, D. *Chem. Rev.* **1992**, *92*, 633.
(32) Wright, J. M.; Landis, C. R.; Ros, M. A. M. P.; Horton, A. D. *Organometallics* **1998**, *17*, 5031.
(33) Landis, C. R.; Luck, L. L.; Wright, J. M. *J. Magn. Reson., Ser. B* **1995**, *109*, 44−59.
(34) Beringhelli, T.; D'Alfonso, G.; Maggioni, D.; Mercandelli, P.; Sironi, A. *Chem. Eur. J.* **2005**, *11*, 650.

even if the arene is different (in nature or in the position of the substituents), in the chlorine derivatives, the substituent on the arene is located between the Cl and NH_2 moiety in both solid state and solution.

Conclusions

From the methodological point of view, the results reported in this paper show the importance of elaborating the D_t data deriving from PGSE NMR measurements through the Stokes−Einstein equation in which the proper *c* factor is introduced (eq 3). The latter, expressed as a function of solvent radius and hydrodynamic radius of the diffusing particles, differs considerable from both 4 (slip boundary conditions) and 6 (stick boundary conditions) for medium-size molecules usually used in organometallic chemistry. Consequently, only by using an appropriate *c* factor can the r_H and V_H values be accurately determined.

The refined PGSE methodology combined with NOE NMR experiments affords a clear picture of the interionic structure of compounds **1**−**3**, which exhibit a remarkable tendency to aggregate, not limited to ion pairing, in a variety of solvents. In fact, for compounds **1** and **2**, ion quadruples that are held together by a [1 × 1] network of intercationic HBs between Ru-Cl and the N-H groups are formed in solution. Interestingly enough, in 2-propanol-d_8, ion quadruples prefer to dissociate into an anion and a "XRuRu$^+$" ion triple rather than into two ion pairs. Compelling evidence for this process comes from the aggregation numbers, N^+ and N^-, determined by PGSE measurements, that agree with those expected for ion triples. Another clue about the "RuRu" approach is derived from interionic NOE experiments that indicate that relative anion−cation orientation is the same in ion pairs, ion triples, and ion quadruples.

Compound **3**, which has no N-H moiety, has a lesser tendency to aggregate than **1** and **2**, even though it also affords ion quadruples in apolar and aprotic solvents probably because it has to reduce the molecular dipole moment in order to stay in solution. In **3**PF_6 the anion location is less specific than in **1**PF_6 and **2**PF_6 as a consequence of the less intimate ion pair due to the absence of NH···FPF_5 HBs.

Finally, the quantitative evaluation of intramolecular NOEs indicates that particular conformations of cymene in **1**−**3** are more abundant than others in solution, and this is mainly determined by steric factors.

Experimental Section

$RuCl_3 \cdot 3H_2O$, ethylenediamine, *N*,*N*′-dimethylethylenediamine, and *N*,*N*,*N*′,*N*′-tetramethylethylenediamine were purchased from Sigma. [Ru(η^6-arene)Cl_2]$_2$ was prepared according to Benneth et al.[35] Compounds **1**−**3** were prepared under nitrogen using standard Schlenk techniques. Solvents were freshly distilled (hexane with Na, Et_2O with Na/benzophenone, MeOH with CaH_2, CH_2Cl_2 with P_2O_5) and degassed, by many gas−pump−nitrogen cycles, before use.

One- and two-dimensional ^{1}H, ^{13}C, ^{19}F, and ^{31}P NMR spectra were measured on Bruker DPX 200 and DRX 400 spectrometers. Referencing is relative to TMS (^{1}H and ^{13}C), CCl_3F(^{19}F), and 85% H_3PO_4 (^{31}P). NMR samples were prepared by dissolving the suitable amount of compound in 0.5 mL of solvent.

Synthesis of Complexes 1−3X.[15] **Synthesis of complex 1BPh$_4$.** [Ru(η^6-arene)Cl_2]$_2$ (0.100 g, 0.163 mmol) was added to a solution of 24 μL (0.360 mmol) of the ethylenediamine in 5 mL of MeOH. The resulting red-orange suspension was stirred for 3 h at rt until it changed into a yellow solution; a large excess of $NaBPh_4$ (10 equiv) dissolved in 0.5 mL of MeOH was added, and a precipitate formed. The solution was filtered and the solid was washed with cold MeOH and *n*-hexane. Yield = 84%. ^{1}H NMR (CD_2Cl_2, 298 K, 400.13 MHz, *J* in Hz): δ 1.26 (d, $^3J_{H7-H6}$ = 6.95, H7), 1.72 (m, H8), 2.01 (m, H8), 2,04 (s, H5), 2.12 (br, H^d), 2.62 (sept, $^3J_{H6-H7}$=7.19 H6), 3.09 (br, H^u), 4.98 (d, $^3J_{H3-H2}$ = 5.95 H3), 5.17 (d, $^3J_{H2-H3}$ = 6.00, H2), 6.96 (t, $^3J_{p-m}$ = 7.19, p), 7.10 (t, $^3J_{m-o,p}$ = 7.36, m), 7.43 (br, o).

Synthesis of Complex 1PF$_6$. Pathway a. [Ru(η^6-arene)Cl_2]$_2$ (0.100 g, 0.163 mmol) was added to a solution of 24 μL (0.360 mmol) of the ethylenediamine in 5 mL of MeOH. The resulting red-orange suspension was stirred for 3 h at rt until it changed into a yellow solution; a large excess of NH_4PF_6 (10 equiv) dissolved in 0.5 mL of MeOH was added, and a precipitate formed. The solution was filtered, and the solid was washed with cold MeOH and *n*-hexane. Yield = 80%. **Pathway b. 1**BPh_4 (0.100 g, 0.154 mmol) was dissolved in 5 mL of CH_2Cl_2. A 0.056 g sample of $TlPF_6$ (0.161 mmol) was added under nitrogen atmosphere, and $TlBPh_4$ precipitated from the solution. The solution was filtered and dried under vacuum, giving a yellow solid. Yield = 98%. ^{1}H NMR (CD_2Cl_2, 298 K, 400.13 MHz, *J* in Hz): δ 1.34 (d, $^3J_{H7-H6}$ = 6.94, H7), 2.28 (s, H5), 2.69 (m, H8 e 8′), 2.87 (sept, $^3J_{H6-H7}$ = 6.83 H6), 3.11 (br, H^d), 4.91 (br, H^u), 5.52 (d, $^3J_{H3-H2}$ = 5.94 H3), 5.67 (d, $^3J_{H2-H3}$ = 6.00, H2). ^{19}F NMR (CD_2Cl_2, 298 K, 376.65, *J* in Hz): δ −75.10 (d, $^1J_{FP}$ = 707.9, PF_6^-)

Synthesis of Complex 2,3X (X = BPh$_4$, PF$_6$). Complexes **2**,**3**X (X = BPh_4, PF_6) were synthesized with the same procedures as **1**X using the appropriate ligand. Yields were in the 85−95% range. **2**BPh_4: ^{1}H NMR (CD_2Cl_2, 298 K, 400.13 MHz, *J* in Hz): δ 1.28 (d, $^3J_{H7'}$-H6 = 7.1, H7′), 1.30 (d, $^3J_{H7-H6}$ = 7.1, H7), 1.85 (m, H9′), 1.95 (m, H8), 2.04 (s, H5), 2.14 (m, H8′), 2.40 (m, H9), 2.61 (d, $^3J_{Me^{u}d^{n}-H^{u}u^{n}}$ = 5.76, Me^d), 2.80 (sept, $^3J_{H6-H7,H7'}$ = 7.0, H6), 2.87 (d, $^3J_{Me^{u}u^{n}-H^{u}d^{n}}$ = 6.19, Me^u), 3.45 (br, H^d), 4.04 (br, H^u), 5.02 (d, $^3J_{H3'-H2'}$ = 6.09, H3′), 5.06 (d, $^3J_{H3-H2}$ = 6.04, H3), 5.14 (d, $^3J_{H2-H3}$ = 2.74, H2), 5.21 (d, $^3J_{H2'-H3'}$ = 5.93, H2′), 6.96 (t, $^3J_{p-m}$ = 7.19, *p*), 7.10(t, $^3J_{m-o,p}$ = 7.36, *m*), 7.43 (br, *o*). ^{13}C{^{1}H} NMR (CD_2Cl_2, 298 K, 100.55 MHz): δ 18.4 (s, C5), 22.1 (s, C7 or C7′), 22.4 (s, C7′ or C7), 31.3 (s, C6), 44.3 (s, Me^d), 45.7 (s, Me^u), 53.2 (s, C8), 57.1 (s, C9), 81.3 (s, C2), 82.1 (s, C2′), 82.7 (s, C3), 82.8 (s, C3′), 86.0 (s, C1), 106.1 (s, C4), 122.4 (s, *p*), 126.1 (q, $^3J_{m-B}$ = 2.7, *m*), 136.3 (d, $^2J_{o-B}$ = 1.4, *o*), 164.4 (q, $^1J_{C-B}$ = 49.2, C-ipso). **2**PF_6: ^{1}H NMR (CD_2Cl_2, 298 K, 400.13 MHz, *J* in Hz): δ 1.33 (d, $^3J_{H7'-H6}$ = 6.92, H7′), 1.34 (d, $^3J_{H7-H6}$ = 6.90, H7), 2.20 (m, H8), 2.34 (s, H5), 2.53 (m, H9′), 2.73 (m, H8′ e H9), 2.88 (d, $^3J_{Me^{u}d^{n}-H^{u}u^{n}}$ = 5.78, Me^d), 2.98 (sept, $^3J_{H6-H7,H7'}$ = 7.0, H6), 3.14 (d, $^3J_{Me^{u}u^{n}-H^{u}d^{n}}$ = 6.21, Me^u), 3.61 (br, H^d), 5.41 (m, H2 e H3), 5.46 (d, $^3J_{H3'-H2'}$ = 6.16, H3′), 5.55 (d, $^3J_{H2'-H3'}$ = 6.03, H2′), 5.61 (br, H^u). ^{19}F NMR (CD_2Cl_2, 298 K, 376.65, *J* in Hz): δ −75.10 (d, $^1J_{FP}$ = 707.9, PF_6^-). **3**BPh_4: ^{1}H NMR (CD_2Cl_2, 298 K, 400.13 MHz, *J* values in Hz): δ 1.30 (d, $^3J_{H7-H6}$ = 6.94, H7), 2.07 (s, H5), 2.18 (m, H8), 2.47 (m, H8), 2.77 (s, Me^d), 3.03 (sept, $^3J_{H6-H7}$ = 7.0, H6), 3.08 (s, Me^u), 5.16 (d, $^3J_{H3-H2}$ = 6.41, H3), 5.27 (d, $^3J_{H2-H3}$ = 6.41, H2), 6.93 (t, $^3J_{p-m}$ = 7.21, *p*), 7.07 (t, $^3J_{m-o,p}$ = 7.34, *m*), 7.37 (br, *o*). **3**PF_6: ^{1}H NMR (CD_3OD, 298 K, 400.13 MHz, *J* in Hz): δ 1.31 (d, $^3J_{H7-H6}$ = 6.88, H7), 2.25 (s, H5), 2.46 (m, H8), 2.57 (m, H8), 2.87 (s, Me^d), 3.08 (sept, $^3J_{H6-H7}$ = 6.79, H6), 3.38 (s, Me^u), 5.49 (d, $^3J_{H2-H3}$ = 5.84, H2), 5.87 (d, $^3J_{H3-H2}$ = 5.71, H3). ^{19}F NMR (CD_3OD, 298 K, 376.65, *J* in Hz): δ −75.10 (d, $^1J_{FP}$ = 707.9, PF_6^-).

***T*$_1$ Measurements.** The longitudinal relaxation times for the ^{1}H nuclei were measured by the standard inversion recovery method on solutions of complexes **1**PF_6 in methylene

(35) Benneth, M. A.; Smith, A. K. *J. Chem. Soc., Dalton Trans*. **1974,** 233.

chloride-d_2 at 296 K. A total of 15 experiments, having the relaxation delay ranging from 0.001 to 15 s, were acquired, each of them consisting of 32 scans. The total relaxation delay between two consecutive scans was 15 s. All single experiments were Fourier transformed. Frequency domain spectra were processed with a standard T_1/T_2 software package available on Bruker spectrometers to extract the relaxation parameters. Important T_1 values are 0.5 s for H^u, 0.6 s for H^d, 2.2 and 2.4 s for 2 and 3, respectively, 0.8 s for 8, 2.2 s for 6, 1.7 for 5-Me, and 1.2 s for 7-*i*Pr.

NOE Measurements. The ^{1}H-NOESY[36] NMR experiments were acquired by the standard three-pulse sequence or by the PFG version.[37] Two-dimensional ^{19}F,^{1}H-HOESY NMR experiments were acquired using the standard four-pulse sequence or the modified version.[38] The number of transients and the number of data points were chosen according to the sample concentration and to the desired final digital resolution. Semiquantitative spectra were acquired using a 1 s relaxation delay and 800 ms mixing times. Quantitative ^{1}H-NOESY and ^{19}F,^{1}H-HOESY NMR experiments were carried out with a relaxation delay of 10 s and a mixing time of 0.15 s (initial rate approximation).[39]

PGSE Measurements. ^{1}H and ^{19}F PGSE NMR measurements were performed by using the standard stimulated echo pulse sequence[40] on a Bruker AVANCE DRX 400 spectrometer equipped with a GREAT 1/10 gradient unit and a QNP probe with a Z-gradient coil, at 296 K without spinning. The shape of the gradients was rectangular, their duration (δ) was 4−5 ms, and their strength (G) was varied during the experiments. All the spectra were acquired using 32K points and a spectral width of 5000 (^{1}H) and 18 000 (^{19}F) Hz and processed with a line broadening of 1.0 (^{1}H) and 1.5 (^{19}F) Hz. The semilogarithmic plots of $\ln(I/I_0)$ vs G^2 were fitted using a standard linear regression algorithm; the R factor was always higher than 0.99. Different values of Δ, "nt" (number of transients), and number of different gradient strengths (G) were used for different samples. For example, for the measurements of **3**PF_6 0.7 mM in methylene chloride-d_2, the "nt" values were 480 (^{1}H) and 960 (^{19}F) with a total acquisition time of 18 (^{1}H) and 24 (^{19}F) h. 5, 7, Me, *o*-H, *m*-H, and fluorine resonances were investigated as usual.

The dependence of the resonance intensity (I) on a constant diffusion time and on a varied gradient strength (G) is described by eq 5:

$$\ln \frac{I}{I_0} = -(\gamma\delta)^2 D_t\left(\Delta - \frac{\delta}{3}\right)G^2 \qquad (5)$$

where I = intensity of the observed spin−echo, I_0 = intensity of the spin−echo without gradients, D_t = diffusion coefficient, Δ = delay between the midpoints of the gradients, δ = length of the gradient pulse, and γ = magnetogyric ratio.

(a) Pure Solvents. The diffusion coefficient D_t, which is directly proportional to the slope of the regression line obtained by plotting $\log(I/I_o)$ vs G^2 (eq 5), was estimated by measuring the proportionality constant using a sample of HDO (0.04%) in D_2O (known diffusion coefficient in the range 274−318 K)[19,41] under the exact same conditions as the sample of interest. From the measured D_t, r_H was determined by introducing into eq 3 the van der Waals radius of the solvent as r_{solv} and the solution viscosity value corrected to take into account both the actual temperature[17] and the deuteration of the solvents.[18]

(b) TMSS Solutions. D_t for TMSS and solvents that are the sample (sa) and the internal standard (st), respectively, were evaluated as described in (a). From eq 1 the ratio of the D_t values for TMSS and solvent, equal to the ratio of the slopes (m) of the straight lines coming from plotting $\log(I/I_o)$ vs G^2, is

$$\frac{m^{sa}}{m^{st}} = \frac{D_t^{sa}}{D_t^{st}} = \frac{c^{st} r_H^{st}}{c^{sa} r_H^{sa}} = f(r_{solv}, r_H^{sa}, r_H^{st}) \qquad (6)$$

The latter circumvents the dependence of the D_t values on temperature, solution viscosity, and gradient calibration. From eq 6 the denominator $c^{sa} r_H^{sa}$ can be determined since the m^{sa}/m^{st} ratio was measured and $c^{st} r_H^{st}$ was evaluated as described in (a). Since c_{sa} depends on r_{solv} and r_H^{sa} according to eq 2 and r_{solv} was measured in point (a), r_H^{sa} was determined graphically solving the equation (Supporting Information)

$$c^{sa} r_H^{sa} = \frac{6}{\left[1 + 0.695\left(\frac{r_{solv}}{r_H^{sa}}\right)^{2.234}\right] r_H^{sa}} \qquad (7)$$

(c) 1−3 Solutions Containing TMSS. D_t for **1**−**3** compounds, TMSS, and solvents were evaluated as described in (a). The correction factor for the ^{19}F-PGSE measurements was $[\gamma(^1H)/\gamma(^{19}F)]^2 = 1.129$. The r_H values for compounds **1**−**3** were estimated as described in (b), but in these cases TMSS and/or the solvent itself served as internal standard.

The van der Waals volume of TMSS was computed from the crystal structures[42] using the software package WebLab ViewerLite 4.0. The volume of ion pairs was determined from the crystal structure of **1**PF_6; for the other complexes, we added the volume of the methyl group according to Bondi's methodology.[6]

The uncertainty in measurement was estimated by determining the standard deviation of m by performing experiments with different Δ values. The standard propagation of error analysis gave a standard deviation of approximately 3−4% in hydrodynamic radii and 10−15% in hydrodynamic volumes and aggregation numbers N.

Acknowledgment. We thank the Ministero dell'Istruzione, dell'Università e della Ricerca (MIUR, Rome, Italy), Programma di Rilevante Interesse Nazionale, Cofinanziamento 2004−2005 for support.

Supporting Information Available: Data of PGSE NMR measurements (Table S1−S27), dependence of N^+ and N^- on the concentration for **3**PF_6 and **3**BPh_4 (Figures S1, S2), dependence of cr_H on r_H in methylene chloride-d_2 (Figure S3), representative two-dimensional experiments for the intramolecular and interionic characterization of compounds **1**−**3** (Figures S4−S8). This material is available free of charge via the Internet at http://pubs.acs.org.

OM050145K

(36) Jeener, J.; Meier, B. H.; Bachmann, P.; Ernst, R. R. *J. Chem. Phys.* **1979**, *71*, 4546.
(37) Wagner, R.; Berger, S. *J. Magn. Reson. A* **1996**, *123*, 119.
(38) Lix, B.; Sönnichsen, F. D.; Sykes, B. D. *J. Magn. Reson. A* **1996**, *121*, 83.
(39) Neuhaus, D.; Williamson, M. *The Nuclear Overhauser Effect in Structural and Conformational Analysis*, Wiley-VCH: Weinheim, 2000; Chapter 4.
(40) Tanner, J. *J. Chem. Phys.* **1970**, *52*, 2523.
(41) Tyrrell, H. J. W.; Harris, K. R. *Diffusion in Liquids*; Butterworth: London, 1984.
(42) Dinnebier, R. E.; Dollase, W. A.; Helluy, X.; Kümmerlen, J.; Sebald, A.; Schmidt, M. U.; Pagola, S.; Stephens, P. W.; Van Smaalen, S. *Acta Crystallogr.* **1999**, *B55*, 1014.